Biosensors and Bioelectronics 147 (2020) 111763

Contents lists available at ScienceDirect

Biosensors and Bioelectronics

journal homepage: http://www.elsevier.com/locate/bios

A novel biosensor for zinc detection based on microbial fuel cell system

Aman Khan [a,1], El-Sayed Salama [b,c,1], Zhengjun Chen [d], Hongyuhang Ni [a], Shuai Zhao [a], Tuoyu Zhou [a], Yaxin Pei [a], Rajesh K. Sani [e], Zhenmin Ling [a], Pu Liu [a,f], Xiangkai Li [a,f,*]

[a] MOE, Key Laboratory of Cell Activities and Stress Adaptations, School of Life Science, Lanzhou University, Lanzhou, 730000, Gansu, PR China
[b] Department of Occupational and Environmental Health, School of Public Health, Lanzhou University, Lanzhou, 730000, Gansu, PR China
[c] Department of Earth Resources and Environmental Engineering, Hanyang University, Seoul, 04763, South Korea
[d] College of Life Science and Technology, Gansu Agricultural University, Lanzhou, 730070, PR China
[e] Department of Chemical and Biological Engineering South Dakota School of Mines and Technology, 501 East St. Joseph Street Rapid City, SD, 57701-3995, USA
[f] Key Laboratory for Resources Utilization Technology of Unconventional Water of Gansu province, Gansu Academy of Membrane Science and Technology, Lanzhou, 730020, Gansu, PR China

ARTICLE INFO

Keywords:
MFC
Zn^{2+} biosensor
Cell permeability
Electron shuttle mediator

ABSTRACT

Microbial fuel cell (MFC) biosensors are self-sustainable device for monitoring of various substrates; however, for heavy metals detection are still scarce. In this study, *E. coli* BL21 was engineered to express the *znt*R, *rib*B, and *opr*F genes with P_{zntA} promoter, which could sense zinc (Zn^{2+}) for riboflavin and porin production. The engineered strain produced high levels of riboflavin (2.4–3.6 μM) and improved cell membrane permeability, with a positive correlation of Zn^{2+} (0–400 μM). The strain was then employed in MFC biosensor under the following operational parameters: external resistance 1000 Ω, pH 9, and temperature 37 °C for Zn^{2+} sensing. The maximum voltages (160, 183, 260, 292, and 342 mV) of the constructed MFC biosensor have a linear relationship with Zn^{2+} concentrations (0, 100, 200, 300, and 400 μM, respectively) ($R^2 = 0.9777$). An Android App was developed for the biosensor system that could sense Zn^{2+} in real-time and *in situ*. The biosensor was applied to wastewater with different Zn^{2+} concentrations and the results showed that the detection range for Zn^{2+} was 20–100 μM, which covers common Zn^{2+} safety standards. The results obtained with developed MFC biosensor were comparable to conventional methods such as colorimetric, flame atomic absorption spectroscopy (FAAS), and inductively coupled plasma optical emission spectroscopy (ICP-OES). In summary, MFC biosensor with biosynthetic strain is an efficient and affordable system for real-time monitoring and sensing of heavy metals.

1. Introduction

Zinc is an abundant transition metal that serves catalytic, structural, redox-modulatory, and regulatory roles owing to its high binding affinity, which is next to that of copper among the Irving-Williams series of metals (Choi et al., 2017). Long term exposure and high dose of Zn^{2+} supplementation and accumulation can cause significant toxicity and is shown to affect digestive and respiratory tracts (Poddalgoda et al., 2019). Therefore, detection of Zn^{2+} in water samples is important for zinc contamination control. The determination of metal concentrations in water by conventional methods such as gas chromatography-mass spectroscopy (GC-MS) (Takeuchi et al., 2019), flame atomic absorption spectroscopy (FAAS) and inductively coupled plasma optical emission spectroscopy (ICP-OES) (Escudero et al., 2010), and inductively coupled plasma-mass spectrometry (ICP-MS) (Ravikumar et al., 2012) have been performed successfully. Despite these analytical methods are expensive, energy-consuming, require pretreated samples (Li et al., 2015), and may not be accessible to rural areas in developing countries (Bereza-Malcolm et al., 2015). A cost-effective and self-sustaining technique needs to be developed for the assessment of metal toxicity in water samples.

A bacterial biosensor is an alternative to analytical methods with reduced cost and labor for detection of metals based on fluorescence proteins or pigment molecules connected to metals sensing operons (regulator) (Cerminati et al., 2015; Choi et al., 2017). Several biosensors have been designed and constructed by employing synthetic biology

* Corresponding author. MOE, Key Laboratory of Cell Activities and Stress Adaptations, School of Life Science, Lanzhou University, Lanzhou, 730000, Gansu, PR China.
E-mail address: xkli@lzu.edu.cn (X. Li).
[1] These authors contributed equally to this work, and can be regarded as co-first author.

https://doi.org/10.1016/j.bios.2019.111763
Received 27 July 2019; Received in revised form 26 September 2019; Accepted 3 October 2019
Available online 5 October 2019

tools for heavy metals (HMs) detection (Kim et al., 2016; Rijavec et al., 2016). Zn^{2+} metal ions are sensed by the zinc regulator ZntR of the MerR and CzrA/SmtB/AztR/ArsR family (Choi et al., 2017; Webster et al., 2014). *E. coli* MC1061 (p*zntRluc*) biosensor detected 2% Zn^{2+} metal ion of the total amount in soil-water extracts (Ivask et al., 2002). *Synechocystis* sp. PCC6803 (p*coaTlux*) monitored 90 % of Zn^{2+} along with Ni^{2+} and Co^{2+} HMs in the soil mixture contaminated with various chemicals and oily wastes (Peca et al., 2008). Detection of Zn^{2+} based on a reporter gene system is of poor sensitivity and not specific (Liu et al., 2012). This system needs an additional signal transducer or external power source with limited detection efficiency (Tanikkul and Pisutpaisal, 2018). Hence, there is a growing demand to develop a system for *in situ* real-time monitoring of HMs toxicity in water.

Microbial fuel cell (MFC) based biosensors are widely used to monitor a broad spectrum of environmental parameters such as biological oxygen demand (Yu et al., 2013), chemical oxygen demand (Su et al., 2011), and organic substrates toxicity (Chen et al., 2016; Kim et al., 2007) in wastewaters. The MFC-based sensor is an advanced system that develops a linear relationship between substrate concentrations and voltages by improving the selectivity and sensitivity of toxicity detection (Yi et al., 2018). Electrons shuttle mediator (riboflavin) facilitated transfer of electrons to increase voltage in MFC (Li et al., 2018; Yang et al., 2015). Flavin biosynthesis genes cluster *rib*-ABCDEHC could synthesize riboflavin and improve MFC performance through the extracellular electron transfer (EET) mechanism (Tao et al., 2015; Yang et al., 2015). However, low membrane permeability of cells of bacterial strains restricted the transfer of electrons from the cells to the electrodes (Liu et al., 2014). *E. coli* has a compact and less permeable outer membrane (OM) with limited electron transfer (Muheim et al., 2017). Overexpression of *opr*F in *E. coli* BL21 enhanced OM permeability and allowed more electrons to get transferred from the OM to the inner membrane and then to the electrode (Yong et al., 2013b).

The present study was conducted to develop a novel, genetically engineered, Zn^{2+}-specific MFC biosensor with *E. coli* BL21 that carried the *rib*B (biosynthetic enzyme 3, 4-dihydroxy-2-butanone-4-phosphate synthase) cognate with P_{zntA} promoter and *opr*F (porin synthetic protein) genes. The constructed biosensor was calibrated for specific operational parameters such as sensitivity, specificity, and stability. The engineered BL21 strain was also investigated for cell membrane permeability and riboflavin synthesis in the MFC. A linear relationship was developed between Zn^{2+} concentrations and electric signals using the engineered BL21 strain as a biosensor in the MFC. Furthermore, the constructed MFC biosensor was compared with conventional methods such as colorimetric, FAAS, and ICP-OES with respect to the detection of Zn^{2+} in wastewater. The constructed MFC biosensor would be a suitable device for real-time monitoring and sensing of HMs in wastewater with a direct electrical output.

2. Materials and methods

2.1. In vitro gene synthesis and plasmid construction

Molecular biological tools were used to construct the plasmids pUC19 and pETDuet-1. The zinc-responsive regulator/promoter (p*znt*R) and riboflavin synthetic (*rib*B) genes were amplified from the genome of *Shewanella oneidensis* MR-1 and porin protein (*opr*F) gene was amplified from *Pseudomonas aeruginosa* using a set of primers with restriction sites. The green fluorescent protein (GFP) gene was present in our laboratory stocks. *znt*R was overlapped with *gfp* and the fragment was digested with *Hind*III and *Bam*HI and inserted into the plasmid pUC19 under the control of the P_{zntA} promoter. The recombinant plasmid was named pUC19-pzntR-GFP and transferred into *E. coli* W-1 for expression. To avoid the high error rate of a long fragment building block, we overlapped the p*znt*R and *rib*B and the resultant fragment was digested with *Bam*HI and *Eco*R1. The digested fragment was ligated downstream of the *opr*F gene under the control of Zn^{2+} inducible promoter P_{zntA}. The resultant plasmid was named pETDuet-1pzntR-ribB-oprF and was transferred into the host strain *E. coli* BL21 (DE3) for expression (Table 1). All gene coding sequences and information were obtained from the NCBI, BioCyc database and screened using PCR. The engineered BL21 strain was cultured in LB medium or M9 medium (1 × M9 medium, 2 mM/L $MgSO_4$, 0.1 mM/L $CaCl_2$, and 0.4% glucose as a carbon source) at 37 °C with shaking at 180 rpm. Ampicillin (50 μg/mL) and IPTG (0.7 mM) were added to the culture medium whenever needed. Engineered cells (1 mL) were grown in 100 mL LB-broth and the culture was incubated at 37 °C in a shaking incubator until OD_{600} reached 0.6.

2.2. Real-time PCR, flow cytometry, and fluorescence microscopy

The expression of pUC19-pzntR-GFP was measured using RT-PCR. The engineered and wild type (WT) *E. coli* W-1 strains were grown in LB-broth at 37 °C to an OD_{600} of 0.6, and different concentrations (0, 30, 60, and 90 μM) of Zn^{2+} were added individually. After 3 h of Zn^{2+} addition, cells were harvested and total RNAs were isolated using the SV total RNA isolation kit (Promega). Quantitative RT-PCR reactions were performed under the following conditions: cDNA synthesis (50 °C, 40 min), denaturation (95 °C, 12 min), and amplification for 40 cycles (95 °C, 20 sec; 60 °C, 1 min). A flow cytometry test was applied, *E. coli* W-1 cells carrying pUC19-pzntR-GFP were cultured with $ZnCl_2$, $NiCl_2$, $CuCl_2$, $HgCl_2$, $CoCl_2$, and $Pb(NO_3)_2$ (final concentration, 90 μM). *E. coli* DH5α containing the empty plasmid was used as a control. A flow cytometer (BD LSRFortessa, USA) equipped with a 488 nm blue solid-state laser was used to observe the cell population at a flow rate of 1 μL/s. For fluorescence microscopy, the engineered cells were induced with Zn^{2+} and harvested after 4 h of centrifugation (3500×*g* for 5 min) at 4 °C. The cells were washed with phosphate-buffered saline (PBS) solution and resuspended in PBS solution supplemented with 0.3% agarose. A fluorescence microscope (Olympus, Japan) with a cooled charge-coupled device camera (B&W SenSys, KAF1401) was used to screen the cells.

2.3. Membrane permeability assay

The membrane permeability of the engineered strain BL21 carrying the recombinant plasmid, pETDuet-1pzntR-ribB-oprF was assessed by o-nitrophenyl-b-galactopyranoside (ONPG) hydrolysis (Arcidiacono et al., 2009). The overnight culture of the engineered BL21strain was inoculated in fresh LB medium. After 5 h of incubation at 37 °C, cells were harvested and washed thrice with PBS buffer (10 mM, pH 7.4). The ONPG hydrolysis assay was performed by mixing 135 mL of ONPG solution (1.5 mM in 10 mM PBS, pH 7.4) with 15 mL of cells suspension. The absorbance of the mixture was measured at 405 nm on a microplate reader (Thermo Scientific, MA, USA). The WT BL21 strain was used as a control and the assay was performed in triplicate.

2.4. MFC design and biosensor operation

A two-chambered MFC operating reactor was set up, each bottle with a working volume of 240 mL divided by proton exchange membrane (PEM; Nafion117, DuPont, USA). The PEM and electrodes were pretreated before use (Chen et al., 2016). Carbon felt as electrodes with an area of 16 cm^2 geometric surfaces were used as anode and cathode. The electrodes were linked with a 1000 Ω external resistor *via* titanium wire. During the MFC operating system, the anode medium was M9 supplemented with the different concentrations (0–400 μM) of Zn^{2+} metal in the interest of the Zn^{2+} responsive regulator. The catholyte was potassium ferricyanide (100 mM potassium ferricyanide in 50 mM phosphate buffer, pH 7.0). The MFC reactor was operated at 37 °C and 180 rpm using a magnetic stirrer. A data acquisition apparatus was used to record the voltage at 10 min intervals in the MFC biosensor. Furthermore, Zn^{2+} concentrations from 0 to 500 μM were also examined in the MFC in different batches. The anode medium was refreshed after 15 h of

Table 1
Oligonucleotide primers, plasmids, and bacterial strains used in this study.

Primers name	Sequence	PCR product
ZntR-F	CGCGGATCCATGTATCGCATTGGTGAGCTG	p*znt*R-operon
ZntR-R	CCGGAATTCACAACCACTCTTAACGCCACTC	
Rib-F	CCCTCGAGGGATGAATCAGACGCTACTTTCCTC	*rib*B-operon
Rib-R	ATTTGCGGCCGCGCTGGCTTTACGCTCATGTG	
OprF-F	CGCGGATCCATGAAACTGAAGAACACCTTAGGC	*opr*F-operon
OprF-R	CCGGAATTCCAACCGATTTCCCTGAGCG	
GFP-F	CGCGGATCCATGAGTAAAGGAGAAGAACTTTTCA	*gfp*-operon
GFP-R	CCCTCGAGTTTGTATAGTTCATCCATGCCATGT	
ZntRrib-F	TTAAGATTGTTGCGCAGGAGATATCGCATTGGTGAGCTGGCAAAAA	p*znt*R-*rib*B-operon
ZntRrib-R	TGCCAGCTCACCAATGCGATATCTCCTGCGCAACAATCTTAACGCAT	
ZntRGFP-F	TGGCGTTAAGAGTGGTTGTATGAGTAAAGGAGAAGAAC	p*znt*R-*gfp*-operon
ZntRGFP-R	AGTTCTTCTCCTTTACTCATACAACCACTCTTAACGCCAC	
QpzntR-F	AAGGCATTGTGCAGGAAAGA	
QpzntR-R	CCACAACAGGCATCGTTAAG	
Plasmids and strains	**Relevant characteristic**	**Source**
pUC19	Clone vector, Amp^R	Laboratory
pET-Duet-1	Clone and expression vector, Amp^R,	Laboratory
pUC19-pzntR-GFP	Recombinant plasmid containing pzntR and GFP	This study
pETDuet-1pzntR-ribB-oprF	Recombinant plasmid containing p*znt*R, *rib*B, and *opr*F genes	This study
S. oneidensis MR-1	Containing p*znt*R and *rib*B genes	Laboratory
P. aerogenosa	Containing *opr*F gene	Laboratory
E. coli DH5α	Clone host strain, containing recombinant plasmid pUC19-pzntR-GFP	This study
E. coli BL21 (DE3)	Expression strain, containing recombinant plasmid pETDuet-1pzntR-ribB-oprF	This study

incubation and the concentration was changed for each batch. The Zn^{2+} concentrations were increased gradually in each batch of operation in the same MFC.

A portable biosensor was developed where the sensor was able to collect voltage signals through a data acquisition card, convert them into digital signals, record, and display real-time signals using Android system App. The software was developed in Android studio with Java language. The collected experimental data was run on the App, which displayed it in the real-time in the form of dynamic graphs. The App was modified form our previous *p*-nitrophenol software (Chen et al., 2016). The signal acquisition software can also calculate the relationship between voltage and Zn^{2+} ions. The developed software has been uploaded to GitHub (https://github.com/maomao0601/CollectingData) (Supplementary materials).

2.5. Optimization parameters for the biosensor test

The constructed sensor strain BL21 was applied in MFC to optimized parameters for working condition. The engineered BL21 strain was grown in different Zn^{2+} concentrations (0–800 μM), temperatures (25, 30, 37, and 45 °C), pH values (5.5, 7.01, 8.02, 9.00, and 11.00), and heavy metals including $ZnCl_2$, $NiCl_2$, $CuCl_2$, $HgCl_2$, $CoCl_2$, and Pb $(NO_3)_2$ at a final concentration of 300 μM supplemented with the M9 medium in the MFC reactor. All experiments were performed in triplicate.

2.6. Application of the constructed MFC biosensor in wastewater

The engineered BL21 sensor strain was applied for practical application in synthetic wastewater. A dual-chambered MFC device (working volume of 240 mL) with synthetic wastewater and M9 fresh medium (1:1) supplemented with 0, 20, 60, and 100 μM of Zn^{2+} concentrations were set up (Cerminati et al., 2015). The concentration was selected based on common Zn^{2+} levels observed in the M9 growth media. Increase in voltage defined the exposure of Zn^{2+} at different concentrations and detection of Zn^{2+} in the MFC reactor was measured by electric signals. The same Zn^{2+} contaminated water was also measured using analytical methods such as colorimetric, FAAS, and ICP-OES and the results were compared with those of the MFC biosensor.

2.7. Analytical methods

Voltage was calculated according to $I = V/R$ (Ohm's law), where I is the current, V is the observed voltage, and R, external resistance, and $P = VI$, where P is power. The anode geometric surface area (16 cm^2) was used for current density (mA m^{-2}) and power density (mW m^{-2}) calculations. Open-circuit voltage (OCV) was maximum voltage where the external resistance is infinite. The external resistance declining from 9999 to 100 Ω was used to determine the polarization curve (Logan, 2009). Riboflavin concentration in the anode electrolyte of the MFC was examined by time course induction using HPLC equipped with a UV detector. The column used was an Agilent analytical C18 (4.6 mm × 105 mm) (Agilent, USA). In detail, 2 mL of the electrolyte samples were collected at 12 h intervals from the MFC reactor and centrifuged (6000 rpm, 5 min). For HPLC analysis, the supernatant was filtrated with a 0.22 μm cellulose membrane and subjected to the system according to the procedure described by Vasilaki et al. (2010). The supernatant (10 μL) was then analyzed with an eluent of 50% methanol and 50% ddH_2O at 1.0 mL/min of flow rate and the HPLC profile was observed at 270 nm.

Cyclic voltammetry (CV) was implemented in a three-electrode configuration with an Ag/AgCl reference electrode with a potentiostat (CHI604E, Shanghai, China). The CV scan rate was 5 mV/s in the range from -0.8–0.8 V (vs SHE). A scanning electron microscope (s-3400, HITACHI, Japan) was used to observe the formation of anode biofilms on an electrode. The experimental data in triplicate was statistically analyzed using mean and standard deviations. All graphs and curve fits were prepared in GraphPad Prism 7 (GraphPad, San Diego, CA, USA) and Origin 8.0 (Origin Lab, Massachusetts, and USA).

3. Results and discussion

3.1. Construction of Zn^{2+} detecting exoelectrogen

To construct the *E. coli* strain that can sense Zn^{2+} and generate electricity, *znt*R, *rib*B, *opr*F, and cognate promoter P_{zntA} were cloned into pUC19 and pETDuet-1 (Fig. 1a). A constructed plasmid named pUC19-pzntR-GFP containing a transcriptionally insulated p*znt*R controlling the expression of GFP. RT-PCR results revealed that the transcription level of the zinc-responsive regulator/promoter was increased to a maximum of 8.5-folds at 90 μM concentration of Zn^{2+} (Fig. 1b). Under

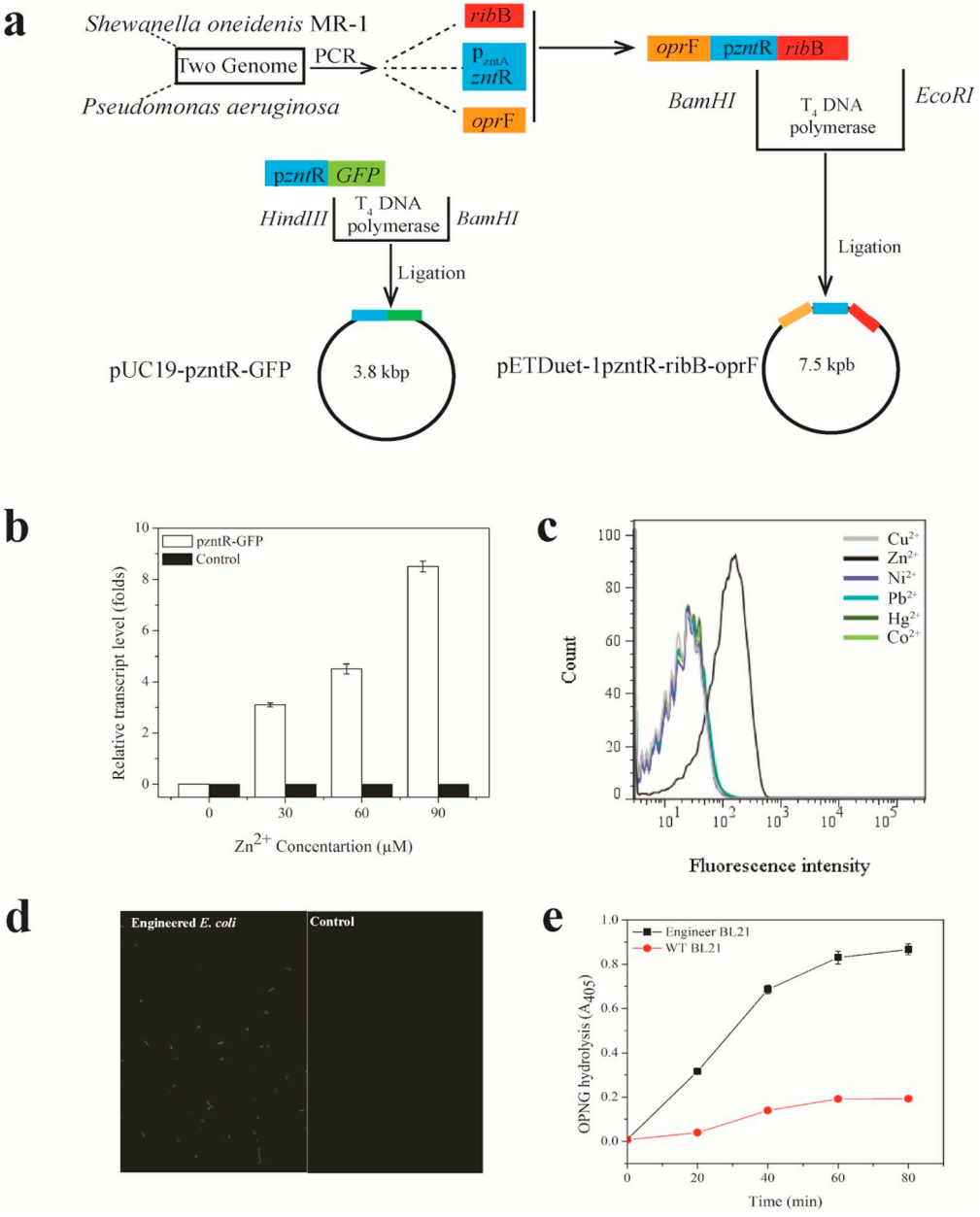

Fig. 1. (**a**) Flowchart of constructed co-expression vector pUC19 and pETDuet-1, (**b**) RT-PCR by using Zn^{2+} concentrations (0, 30, 60, 90 μM), (**c**) Flow cytometry of different metal ions (Cu^{2+}, Zn^{2+}, Ni^{2+}, Pb^{2+}, Hg^{2+} and Co^{2+}) at 90 μM of final concentration, (**d**) Fluorescence microscopy profiles of *E.coli* W-1 carrying the recombinant plasmid pUC19-pzntR-GFP and control, and (**e**) Cell permeability of engineered strain BL21 carried recombinant plasmid pETDuet-1pzntR-ribB-oprF.

the supplementation of different metals ions, the flow cytometry results showed that the constructed Zn^{2+} sensor was highly responsive to Zn^{2+} ion and not sensitive to other divalent metals, such as Cu^{2+}, Ni^{2+}, Pb^{2+}, Hg^{2+}, and Co^{2+} (Fig. 1c). Data from fluorescence microscopy showed that the Zn^{2+} inducible promoter up-regulated downstream genes and synthesize green fluorescence protein (Fig. 1d). This data confirmed that Zn^{2+} metal induces pzntR expression. Then, the GFP gene was replaced by *rib*B and cloned along with *opr*F into the pETDuet-1 plasmid. The recombinant plasmid was transferred to the *E. coli* BL21 for expression. The transformant showed that the *opr*F expression in the engineered strain BL21 increased the cell membrane permeability, which was 4.5 times higher than that of the WT BL21 strain (control) carrying the vacant plasmid (Fig. 1e).

Metal-responsive regulatory units originating from bacterial species have been used in metal biosensors such as MerR or ArsR/SmtB-like regulators (Cerminati et al., 2011; Webster et al., 2014). A whole-cell Zn^{2+}-specific bacterial biosensor has been developed for monitoring of Zn^{2+} ions in human serum showed that the p*znt*A regulator/promoter was up-regulated at a lower range of 20 μM of Zn^{2+} (Watstein and Styczynski, 2018). p*zit*B is a Zn^{2+} responsive regulator/promoter and the relative expression was 5.6-fold at 100 μM of Zn^{2+} (Choi et al., 2017), which was consistent with the present study that showed 8.5-folds transcriptional level of p*znt*R at 90 μM of Zn^{2+}. Transfer of electrons *via* the OM of electrochemically active bacteria to the electrode was restricted due to the dense and strong layer of lipopolysaccharide on the surface cover (Wen et al., 2011; Yong et al., 2014). Overexpression of *opr*F enhanced 4.5 times OM permeability of engineered strain (Fig. 1e).

The obtained results were accordingly to Yong et al. (2013b) by expressing *opr*F in *E. coli* BL21 which increased OM permeability 3.2 times as compared to that by the control strain. These data indicated that p*znt*R, *rib*B, and *opr*F were successfully over-expressed and facilitated the movement of inward electrons outward during EET mechanism in

constructed Zn^{2+} specific sensor.

3.2. Linear relationship between Zn^{2+} concentrations and voltage generation

The constructed Zn^{2+} sensing strain was applied in a two-chambered MFC with different concentrations of Zn^{2+} and the voltage output was monitored. The maximum voltage generation (160, 183, 260, 292, and 342 mV) was correlated with the Zn^{2+} concentrations (0, 100, 200, 300, and 400 μM, respectively) (Fig. 2a). A significant linear relationship between Zn^{2+} concentrations and the maximum voltage of the constructed MFC biosensor was observed ($R^2 = 0.9777$) (Fig. 2b). Moreover, the amendment of Zn^{2+} concentrations at different batches led to an increase in voltage generation from 98 mV to 189 mV at 0–400 μM using the engineered BL21 strain (Fig. 2c). Increasing Zn^{2+} concentration to 500 μM inhibited the voltage generation. Riboflavin is a key factor in promoting MFC voltage generation. Maximum riboflavin production in the anolyte was observed from 2.41 μM/L to 3.6 μM/L at 100–400 μM of Zn^{2+} concentrations within 120 h of incubation, while there was no flavin production observed at 0 concentration of Zn^{2+} (Fig. 2d). The results suggested that the *rib*B gene induces by Zn^{2+} responsive promoter and elevated the voltage generation in MFC. This data indicated that the constructed MFC biosensor enabled the cell to respond to Zn^{2+} in a dose-dependent manner and synthesize flavins in the MFC.

Zn^{2+} specific biosensor *P. putida* X4 (pczcR3GFP) was fabricated by fusing *egfp* with *czc*R3 promoter which showed a relative relationship between Zn^{2+} concentrations and fluorescence intensity in a range (5–55 μmol/L) of Zn^{2+} in soil extract (Liu et al., 2012). The correlation between Zn^{2+} concentrations (100–1000 μM) and relative fluorescence was found linear by employing *E. coli* carried *zra*P and GFP in LB media (Ravikumar et al., 2011). Zn^{2+} sensor based on pigment molecule response responded to Zn^{2+} in the range of 10, 20, and 100 μM in human serum (Watstein and Styczynski, 2018). Detection of Zn^{2+} by fluorescence measurement is not suitable for real-time monitoring; however, this drawback was overcome using the MFC-based biosensor. An arsenic (*pars*R) specific biosensor constructed in *S. onidensis* MR-1 strain showed a linear relationship at 0–100 μM of arsenic concentrations with the maximum current peak ranging from 10 μA to 40 μA in the bioelectrochemical system (Webster et al., 2014). This was consistent with the present study where a correlation curve was observed between Zn^{2+} concentrations and voltages $R^2 = 0.9777$. Detection of benzoylecgonine in urine-based wastewater examined in batch MFC showed that increasing concentrations of benzoylecgonine (0–3.45 μM) led to decline the voltage from 0.31 V to 0.26 V (Catal et al., 2019). In contrast, detection of Zn^{2+} in batch MFC was associated with electricity generation assisted by riboflavin production. The genes cluster, *rib*ABCDE inserted in *E. coli* BL21 can increase voltage by 9.6-fold than that present in the control by producing riboflavin in anode MFC (Tao et al., 2015). *S. oneidensis* carrying *rib*ADEHC genes cluster could synthesize 25.7 μM/L of riboflavin and produce 13.2-fold of voltage (Yang et al., 2015). The results indicated that the voltage alteration was directly related to the quantity of Zn^{2+} in the medium that showed the bio-sensing capability and sensitivity of the engineered BL21 strain.

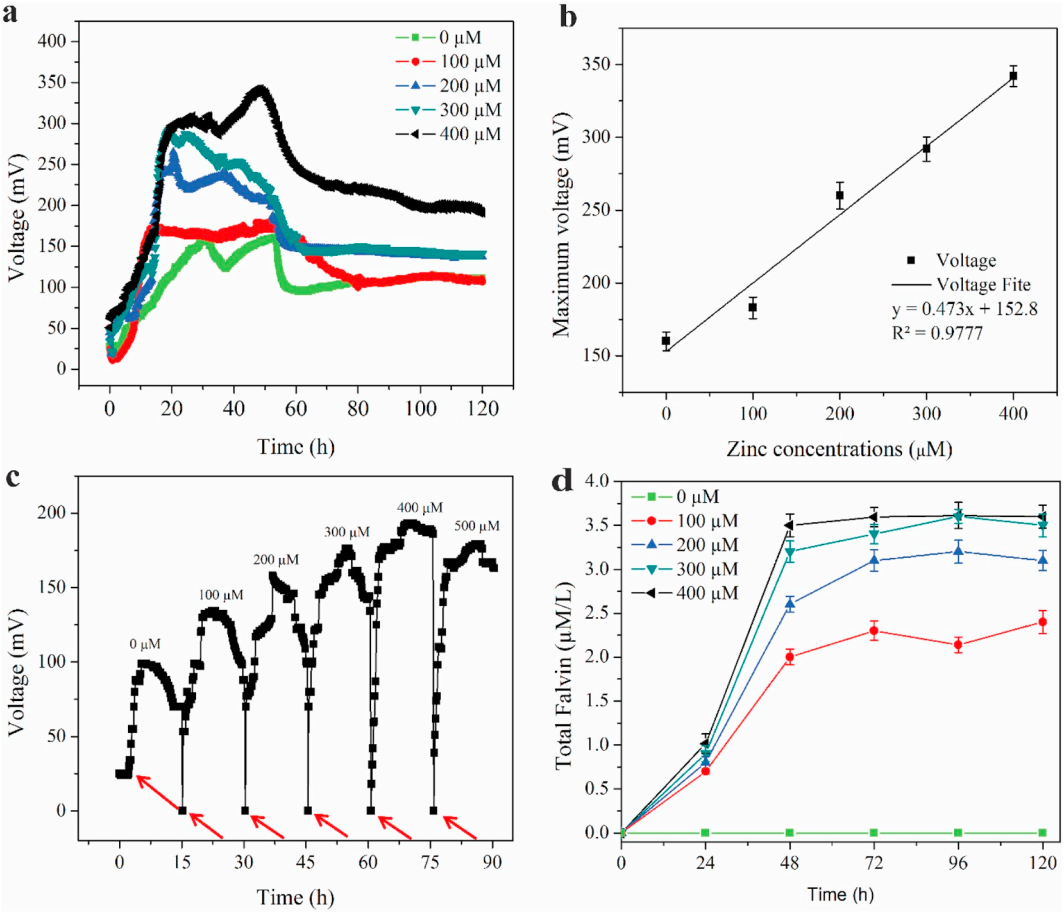

Fig. 2. **(a)** Voltage generation by engineered BL21 strain at different concentrations of Zn^{2+} from 0 to 400 μM, **(b)** A linear relationship curve between the maximum voltage and Zn^{2+} concentrations, **(c)** biofilm based MFC in different batches. Arrows indicate the addition of fresh media, **(d)** riboflavin production at a different time interval.

3.3. Influence of different environmental parameters on constructed Zn^{2+} sensor in MFC

The constructed sensor strain was applied for practical applications under the various environmental parameters for optimization in MFC. The results revealed that the maximum voltage was generated by the MFC biosensor enhanced from 158 mV to 341 mV at 0–400 μM of Zn^{2+} concentrations (Fig. 3a) and showed a linear relationship ($R^2 = 0.9882$) among these parameters (Fig. 3b). Electricity generation decreased from 341 mV to 240 mV at 600 and 800 μM of Zn^{2+}. This indicated that voltage established a linear relationship with Zn^{2+} concentrations which ensures the sensitivity and selectivity of the constructed MFC biosensor. It was also observed that a temperature of 37 °C is suitable for the growth of the engineered BL21 strain (Fig. 3c). When the temperature increased to 45 °C, voltage output significantly reduced because of the growth inhibition of engineered strain (Fig. 3d). For the metal ions, the

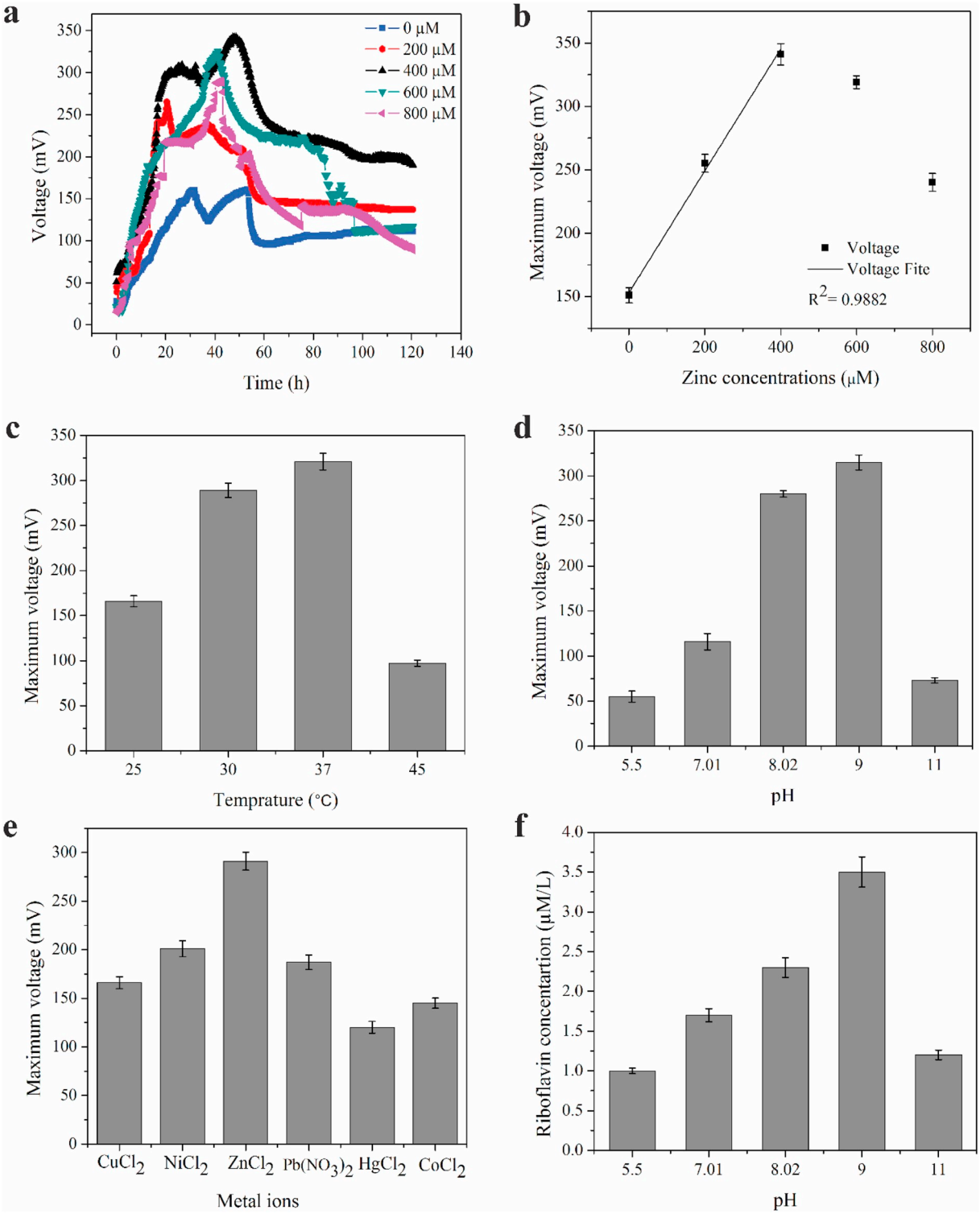

Fig. 3. (**a**) Optimization of parameters for Zn^{2+} constructed sensor at different concentrations of Zn^{2+}, (**b**) maximum voltage output, (**c**) temperatures, (**d**) pH, (**e**) metals ions, and (**d**) riboflavin production at different pH in MFC.

maximum voltage was observed with the Zn^{2+} ion and produced high concentrations of riboflavin at pH 9 (Fig. 3e and f). Concerning interference tests, the constructed MFC biosensor did not show any response to Cu^{2+}, Ni^{2+}, Pb^{2+}, Hg^{2+}, and Co^{2+} metals. The constructed biosensor targeting Zn^{2+}metal ion is the forefront in MFC biosensor design.

To monitor the toxicity in the MFC biosensor, a series of constructional and operational parameters such as pH, temperature, and contaminant concentrations were considered important factors which directly impact voltage generation and sensor sensitivity (Chen et al., 2016; Yi et al., 2019). A good correlation between voltages and Zn^{2+} concentrations at 0–400 μM was developed while increasing Zn^{2+} concentration up to 600 μM declined the voltage in the MFC (Fig. 3a). The similar results were reported by Chen et al. (2016) detecting *p*-nitrophenol (PNP) in wastewater has linear relations at 50–200 mg/L and the voltage was inhibited by increasing PNP concentration to 300 mg/L. The linear correlation curve between voltages and glucose concentrations (0–400 mg/L) was also observed in the MFC biosensor (Yu et al., 2017). Maximum voltage and riboflavin production were observed under environmental parameters as follows: Zn^{2+} concentration, 400 μM; pH 9; and temperature, 37 °C (Fig. 3).

The obtained results were in accordance with the previous reports that acidification restricted the biofilm formation, community alteration, and bacterial growth in MFCs (Patil et al., 2010; Xu et al., 2016), and alkaline pH significantly increases the synthesis of riboflavin in MFC by *S. oneidensis* MR-1 (Yong et al., 2013a; You et al., 2018). Most of the previously constructed biosensors were not specific in response to several other divalent metals. However, the Zn^{2+} specific sensor based on the reporter gene was constructed by (Liu et al., 2012), while the present biosensor is based on the MFC. This data indicated that 37 °C and pH 9 were considered as the operating temperature and pH for the detection of Zn^{2+} ranging from 0 μM to 400 μM in the constructed MFC biosensor.

3.4. Electrochemical characteristics of the constructed MFC biosensor

The maximum power density of the engineered BL21 strain reached 75 mW/m^2, which was 6.25 times higher than that of the control (12 mW/m^2). Voltage generation of the engineered BL21 strain in the open circuit was 430 mV, while the WT BL21 strain showed only 220 mV of voltage output (Fig. S1a). A pair of redox peaks of the currents by the engineered strain BL21 was much higher than that of the WT strain (Fig. S1b). In addition, SEM images confirmed that both engineered and WT BL21 strains can form biofilms on carbon felts (Figs. S1c and d). The engineered BL21 strain displayed considerable electrochemical activity in comparison to the control.

Electrochemical tensions in the MFC are related to the secretion of mediator byproducts *via* a permeable outer membrane which can promote MFC performance (Patil et al., 2010). Redox mediators work as a flexible terminal to accept and transfer electrons in the MFC (Kotloski and Gralnick, 2013), such as hydroquinone secreted by *E. coli* that can efficiently enhance the maximum power density to 1300 mW/m^2 (Qiao et al., 2008). In this study, the engineered BL21 strain secreted riboflavin in anode MFC and increased cell membrane permeability which increased the power density by 6.25 times as compared to the control. The obtained results were consistent with that the overexpression of the *rib*ABCDE gene cluster in *S. oneidensis* enhancing power density to 13.2 times higher than its parental strain (Yang et al., 2015). *opr*F expressed in *E. coli* BL21 could significantly improve the membrane permeability and power density by applying exogenous riboflavin (Yong et al., 2013b). This data suggested that the engineered strain produced electroactive compounds in the MFC that promoted the voltage output.

3.5. MFC biosensor cross-validation with analytical methods

The constructed MFC biosensor was tested by feeding the system with wastewater for practical application and cross-validation with the conventional approaches. The results showed that Zn^{2+} specific MFC biosensor has promising sensitivity to 0, 20, 60, and 100 μM of Zn^{2+} concentrations by generating voltages of 78, 92, 146, and 201 mV, respectively (Table S1). Detection of Zn^{2+} concentrations in the wastewater was also analyzed by colorimetric, FAAS, and ICP-OES methods. The results showed that there was no significant difference in the determination of Zn^{2+} between analytical approaches and the MFC biosensor (Fig. 4). The Zn^{2+} biosensor toward standardization in comparison with analytical methods is cost-effective, has a sharp response, and a short life cycle. This data indicated that the water containing Zn^{2+} monitored by the MFC-based biosensor is an economical approach.

Conventionally water quality monitoring by analytical approaches has a widespread use with significant limitations. The conventional methods need experts to operate the equipment, is often expensive, and time-consuming (Li et al., 2015), and the measured contaminant concentrations of water quality do not readily reveal the definite response to humans or other organisms (Jiang et al., 2018).

To address this issue, MFC biosensors function based on biological processes using living organisms and could be implemented as a supplementary tool for water quality assessment. An overview of Zn^{2+} detection in water by the constructed MFC biosensor in comparison to that by the conventional approaches in terms of limit of detection and system cost is presented in Table 2. The MFC-based biosensors are a self-sustaining and cost-efficient device for *in-situ* and online monitoring of metals in the water that avoids difficult laboratory protocols and sample pre-treatment. It has the ability to interact rapidly with the toxic compounds, providing a direct estimation of toxicity and has a long period of operation and less maintenance compared to the analytical systems (Yu et al., 2017). Zinc ions enter into the water from various sources such as pharmaceutical, agricultural, and industrial waste, which is a challenging issue (Liu et al., 2019). The limited detection range of Zn^{2+} by our constructed MFC biosensor was from 20 μM in water and matched the standard zinc concentrations limit in the drinking water of 3 mg/L or 45.8 μM as described by the FAO and WHO, respectively (Noulas et al., 2018), and 15.4 μM according to the legislation in China (Liu et al., 2012). The Environmental Protection Agency (EPA) prescribed that 5 mg/L or 30 μM of zinc is toxic to the environment (Ravikumar et al., 2011), was covered by our constructed MFC biosensor. This approach is a new development in MFC biosensor research for monitoring of metal ions in water or the aquatic environment. However, the applications of MFC biosensors are still in the early stages in the detection of metals and have not been commercialized. Substantial research progress has been achieved on the various aspects, including sensitivity, selectivity, real-time monitoring, and cost-effectiveness while some parameters still influence the performance of MFC biosensor. At present, the MFC biosensor is a cheap method developed for the detection of metals

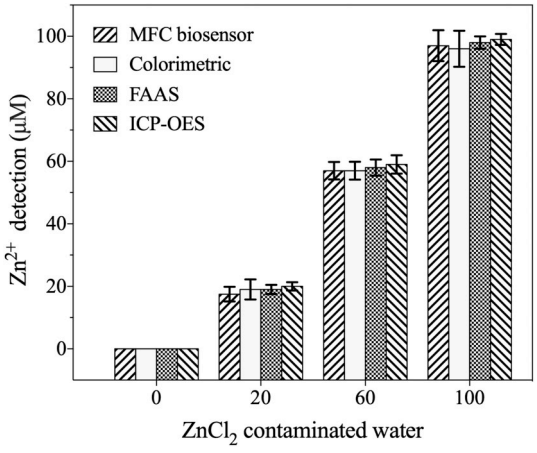

Fig. 4. Comparison of Zn^{2+} detection in wastewater by MFC biosensor with conventional methods (Colorimetric, FAAS, and ICP-OES).

Table 2
Comparison of Zn^{2+} detection by MFC biosensor with analytical methods in wastewater in cost and limited detection range.

Conventional methods	Detection principles	Sources of water	Limited detection (μM)	System setup cost ($)	References
Electrothermal atomic absorption spectroscopy (EAAS)	Atomic absorption	Irrigation water	0.0037	75k	Terres-Martos et al. (2002)
Flame atomic absorption spectroscopy (FAAS)	Atomic absorption	Runoff water	0.12	50k	Legret and Pagotto, (1999)
Graphite furnace atomic absorption spectroscopy (GFAAF)	Atomic absorption	Seawater	0.02	75k	Locatelli1 et al. (1999)
Inductively coupled plasma mass spectroscopy (ICP-MS)	Atomic Emission	Mineral water	.00076	100k	(Misund et al. (1999)
Inductively coupled plasma optical emission spectroscopy (ICP-OES)	Atomic Emission	Natural water	0.8	100k	Escudero et al. (2010)
Differential plus anodic stripping voltammetry (DPASV)	Voltammetry	Sediment-water	3.52	25k	(Legret and Pagotto (1999)
Colorimetric (Silica nanoparticles)	Fluorescence	Ground rainwater	10	1.5K	(Pham et al. (2013)
Microbial fuel cell (MFC) biosensor	Voltage	Synthetic wastewater	20	0.5k	This study

compared to the conventional approaches and the potential for research toward further innovation is encouraging.

4. Conclusions

Zinc responsive regulator (p*znt*R) with *rib*B and *opr*F were collectively expressed in the *E.coli* BL21 strain and make it exoelectrogen. MFC biosensor device based on the Android App system developed by employing the engineered BL21 sensor strain revealed a high specificity to Zn^{2+} and established a good linear relationship between different Zn^{2+}concentrations and voltages output. The constructed MFC biosensor detected 20 μM of Zn^{2+} in water which covers the safety standard of Zn^{2+} in drinking water. It is self-powered, affordable, and is an alternative to conventional methods for the detection of metals in water. This MFC-based biosensor is the first Zn^{2+} biosensor of its kind and future applications need to be explored.

Declaration of competing interest

The authors declare that they have no known competing financial interests or personal relationships that could have appeared to influence the work reported in this paper.

CRediT authorship contribution statement

Aman Khan: Conceptualization, Methodology, Data curation, Investigation, Formal analysis, Writing - review & editing, Writing - original draft, Software, Data curation. **El-Sayed Salama:** Conceptualization, Methodology, Data curation, Investigation, Formal analysis, Writing - review & editing, Funding acquisition, Project administration, Supervision. **Zhengjun Chen:** Software, Data curation. **Hongyuhang Ni:** Writing - original draft. **Shuai Zhao:** Software, Data curation. **Tuoyu Zhou:** Software, Data curation. **Yaxin Pei:** Writing - review & editing. **Rajesh K. Sani:** Writing - review & editing. **Zhenmin Ling:** Writing - review & editing. **Pu Liu:** Funding acquisition, Project administration, Supervision. **Xiangkai Li:** Conceptualization, Methodology, Data curation, Investigation, Formal analysis, Writing - review & editing, Funding acquisition, Project administration, Supervision.

Acknowledgments

The present study was financed by Fundamental Research Funds for the Central Universities grant (lzujbky-2017-br01) and Gansu province major science and technology projects (17ZD2WA017), and National Natural Science Foundation of China Grant (31870082). This work was also supported by the Ministry of Higher Education, Kingdom of Saudi Arabia (KSA) through a grant (PCSED-008-18, 534000-055000018), under the Promising Center for Sensors and Electronic Devices (PCSED), Najran University, KSA.

Appendix A. Supplementary data

Supplementary data to this article can be found online at https://doi.org/10.1016/j.bios.2019.111763.

References

Arcidiacono, S., Soares, J.W., Meehan, A.M., Marek, P., Kirby, R., 2009. J. Pept. Sci. 15 (6), 398–403.
Bereza-Malcolm, L.T., Mann, G., Franks, A.E., 2015. ACS synth. bio. 4 (5), 535–546.
Catal, T., Kul, A., Atalay, V.E., Bermek, H., Ozilhan, S., Tarhan, N., 2019. J. of P. Sour. 414, 1–7.
Cerminati, S., Soncini, F.C., Checa, S.K., 2011. Biotech. and bioeng 108 (11), 2553–2560.
Cerminati, S., Soncini, F.C., Checa, S.K., 2015. Chem. Commun. 51 (27), 5917–5920.
Chen, Z., Niu, Y., Zhao, S., Khan, A., Ling, Z., Chen, Y., Liu, P., Li, X., 2016. Biosens. Bioelectron. 85, 860–868.
Choi, S.H., Lee, K.L., Shin, J.H., Cho, Y.B., Cha, S.S., Roe, J.H., 2017. Nat. Commun. 8, 15812.
Escudero, L.A., Martinez, L.D., Salonia, J.A., Gasquez, J.A., 2010. Micro. J. 95 (2), 164–168.
Ivask, A., Virta, M., Kahru, A., 2002. Soil bio. & biochem. 34 (10), 1439–1447.
Jiang, Y., Yang, X., Liang, P., Liu, P., Huang, X., 2018. Rene. and Sust. En. Rev. 81, 292–305.
Kim, H.J., Lim, J.W., Jeong, H., Lee, S.J., Lee, D.W., Kim, T., Lee, S.J., 2016. Biosens. Bioelectron. 79, 701–708.
Kim, M., Sik Hyun, M., Gadd, G.M., Joo Kim, H., 2007. J. Environ. Monit. 9 (12), 1323–1328.
Kotloski, N.J., Gralnick, J.A., 2013. mBio 4 (1).
Legret, M., Pagotto, C., 1999. Sci. Total Environ. 235 (1–3), 143–150.
Li, L., Liang, J., Hong, W., Zhao, Y., Sun, S., Yang, X., Xu, A., Hang, H., Wu, L., Chen, S., 2015. Enviro. sci. technol. 49 (10), 6149–6155.
Li, M., Zhou, M., Tian, X., Tan, C., McDaniel, C.T., Hassett, D.J., Gu, T., 2018. Biot. adv. 36 (4), 1316–1327.
Liu, P., Huang, Q., Chen, W., 2012. Environ. Pollut. 164, 66–72.
Liu, Y., Wang, Z., Liu, J., Levar, C., Edwards, M.J., Babauta, J.T., Kennedy, D.W., Shi, Z., Beyenal, H., Bond, D.R., Clarke, T.A., Butt, J.N., Richardson, D.J., Rosso, K.M., Zachara, J.M., Fredrickson, J.K., Shi, L., 2014. Environ Microbiol Rep 6 (6), 776–785.
Liu, Z., Chen, B., Li, X., Wang, L.A., Xiao, H., Liu, D., 2019. Sci. Total Environ. 670, 433–438.
Locatelli1, C., Astara, A., Vasca, E., Campanella, V., 1999. Enviro. monitor. and asses. 58 (23–37).
Logan, B.E., 2009. Nat. Rev. Microbiol. 7 (5), 375–381.
Misund, A., Frengstad, B., Siewers, U., Reimann, C., 1999. Sci. Total Environ. 243–244, 21–41.
Muheim, C., Gotzke, H., Eriksson, A.U., Lindberg, S., Lauritsen, I., Norholm, M.H.H., Daley, D.O., 2017. Sci. Rep. 7 (1), 17629.
Noulas, C., Tziouvalekas, M., Karyotis, T., 2018. J. Trace Elem. Med. Biol. 49, 252–260.
Patil, S.A., Harnisch, F., Kapadnis, B., Schroder, U., 2010. Biosens. Bioelectron. 26 (2), 803–808.
Peca, L., Kos, P.B., Mate, Z., Farsang, A., Vass, I., 2008. FEMS Microbiol. Lett. 289 (2), 258–264.
Pham, V.D., Ravikumar, S., Lee, S.H., Hong, S.H., Yoo, I.K., 2013. Bioproc. Biosyst. Eng. 36 (9), 1185–1190.
Poddalgoda, D., Macey, K., Hancock, S., 2019. Regul. Toxicol. Pharmacol. 106, 178–186.
Qiao, Y., Li, C.M., Bao, S.J., Lu, Z., Hong, Y., 2008. Chem. comm. (11), 1290–1292.
Ravikumar, S., Ganesh, I., Yoo, I.-k., Hong, S.H., 2012. Process Biochem. 47 (5), 758–765.
Ravikumar, S., Yoo, I.K., Lee, S.Y., Hong, S.H., 2011. Bioproc. Biosyst. Eng. 34 (9), 1119–1126.

Rijavec, T., Zrimec, J., Oven, F., Viršek, M.K., Somrak, M., Podlesek, Z., Gostinčar, C., Leedjärv, A., Virta, M., Tratnik, J.S., Horvat, M., Lapanje, A., 2016. Geomicrobiol. J. 34 (7), 596–605.
Su, L., Jia, W., Hou, C., Lei, Y., 2011. Biosens. Bioelectron. 26 (5), 1788–1799.
Takeuchi, A., Namera, A., Sakui, N., Yamamoto, S., Yamamuro, K., Nishinoiri, O., Endo, Y., Endo, G., 2019. J. Occup. Health 61 (1), 82–90.
Tanikkul, P., Pisutpaisal, N., 2018. Int. J. of Hydr.En. 43 (1), 483–489.
Tao, L., Wang, H., Xie, M., Thia, L., Chen, W.N., Wang, X., 2015. Chem. Commun. 51 (61), 12170–12173.
Terres-Martos, C., Navarro-Alarcon, M., Martin-Lagos, F., Gimenez-Martinez, R., Lopez-Garcia De La Serrana, H., Lopez-Martinez, M.C., 2002. Water Res. 36 (7), 1912–1916.
Vasilaki, A.T., McMillan, D.C., Kinsella, J., Duncan, A., O'Reilly, D.S., Talwar, D., 2010. Clin. Chim. Acta 411 (21–22), 1750–1755.
Watstein, D.M., Styczynski, M.P., 2018. ACS synth. bio. 7 (1), 267–275.
Webster, D.P., TerAvest, M.A., Doud, D.F., Chakravorty, A., Holmes, E.C., Radens, C.M., Sureka, S., Gralnick, J.A., Angenent, L.T., 2014. Biosens. Bioelectron. 62, 320–324.
Wen, Q., Kong, F., Ma, F., Ren, Y., Pan, Z., 2011. J. of P. Sour. 196 (3), 899–904.
Xu, Y.S., Zheng, T., Yong, X.Y., Zhai, D.D., Si, R.W., Li, B., Yu, Y.Y., Yong, Y.C., 2016. Bioresou. technol. 211, 542–547.
Yang, Y., Ding, Y., Hu, Y., Cao, B., Rice, S.A., Kjelleberg, S., Song, H., 2015. ACS Synth. Biol. 4 (7), 815–823.
Yi, Y., Xie, B., Zhao, T., Li, Z., Stom, D., Liu, H., 2019. Bioelectrochemistry 125, 71–78.
Yi, Y., Xie, B., Zhao, T., Liu, H., 2018. Bioresou. technol. 265, 415–421.
Yong, X.Y., Shi, D.Y., Chen, Y.L., Feng, J., Xu, L., Zhou, J., Wang, S.Y., Yong, Y.C., Sun, Y. M., OuYang, P.K., Zheng, T., 2014. Bioresou. technol. 152, 220–224.
Yong, Y.C., Cai, Z., Yu, Y.Y., Chen, P., Jiang, R., Cao, B., Sun, J.Z., Wang, J.Y., Song, H., 2013. Bioresou. technol. 130, 763–768.
Yong, Y.C., Yu, Y.Y., Yang, Y., Liu, J., Wang, J.Y., Song, H., 2013. Biotech. and bioeng. 110 (2), 408–416.
You, L.X., Liu, L.D., Xiao, Y., Dai, Y.F., Chen, B.L., Jiang, Y.X., Zhao, F., 2018. Bioelectrochemistry 119, 196–202.
Yu, D., Bai, L., Zhai, J., Wang, Y., Dong, S., 2017. Talanta 168, 210–216.
Yu, D., Zhai, J., Yong, D., Dong, S., 2013. Analyst 138 (11), 3297–3302.